Eur. Phys. J. E **27**, 345–356 (2008)
DOI 10.1140/epje/i2008-10384-5

THE EUROPEAN PHYSICAL JOURNAL E

Upward penetration of grains through a granular medium

Z.M. Jakšić[1], S.B. Vrhovac[1,a], B.M. Panić[1], Z. Nikolić[2], and B.M. Jelenković[1]

[1] Institute of Physics, P.O. Box 68, Zemun 11080, Belgrade, Serbia
[2] Faculty of Physics, University of Belgrade, Belgrade, Serbia

Received 19 March 2008 and Received in final form 19 August 2008
Published online: 18 November 2008 –

Abstract. We study experimentally the creeping penetration of guest (percolating) grains through densely packed granular media in two dimensions. The evolution of the system of the guest grains during the penetration is studied by image analysis. To quantify the changes in the internal structure of the packing, we use Voronoï tessellation and a certain *shape factor* which is a clear indicator of the presence of different underlying substructures (domains). We first consider the impact of the effective gravitational acceleration on upward penetration of grains. It is found that the higher effective gravity increases the resistance to upward penetration and enhances structural organization in the system of the percolating grains. We also focus our attention on the dependence of the structural rearrangements of percolating grains on some parameters like polydispersity and the initial packing fraction of the host granular system. It is found that the anisotropy of penetration is larger in the monodisperse case than in the bidisperse one, for the same value of the packing fraction of the host medium. Compaction of initial host granular packing also increases anisotropy of penetration of guest grains. When a binary mixture of large and small guest grains is penetrated into the host granular medium, we observe size segregation patterns.

PACS. 45.70.-n Granular systems – 45.70.Mg Granular flow: mixing, segregation and stratification – 47.57.Gc Granular flow

1 Introduction

Granular materials are assemblies of classical macroscopic particles with short-range repulsive interactions. Such systems have attracted considerable interest among engineers and more recently physicists, motivated by fundamental issues such as the relations between microscopic grain interactions and macroscopic properties as well as by practical needs in civil engineering and industrial applications. Granular systems are highly dissipative and exhibit a host of interesting and sometimes counter-intuitive properties [1]. The phenomena studied have included rapid flow regime [2], dense granular flow down an inclined plane [3–6], slowly sheared granular flow [7,8], mixing and segregation in rotating drums [9] and vibrating beds [10,11], and granular compaction under vertical tapping [12–16].

Interparticle contact friction, packing density, and polydispersity are known to be major contributors to the granular packing resistance to deformation [17]. For example, when a flat plate pushes vertically into granular medium the force opposing the plate (penetration resistance) increases with an increase in the degree of polydispersity, packing density and interparticle friction. Moreover, penetration studies can provide an excellent probe of the structure of local jamming and the dynamics of the failure of a jammed state [18].

The present work is focused on a different, but related problem. We are interested in the problem of the upward penetration of guest (percolating) particles due to external force through a host granular packing. We investigate experimentally a two-dimensional (2D) dense, disordered granular medium composed of rigid noncohesive grains. Our experimental apparatus is adapted from a geometry introduced by Kolb *et al.* [19]. Guest grains are injected through the small hole on the bottom boundary of a containing vessel. The external forces applied to the guest grains are large enough to unjam initially static host packing, but the driving is slow enough to stay in quasistatic flow regime.

Of particular interest is the response of dense disordered granular media to a small perturbation induced by the displacement of one of the grains (the "intruder") [19–23]. Kolb *et al.* [22] analyzed experimentally the evolution of the response to this perturbation by considering the coarse-grained displacement field, as well as the mean packing fraction and coordination number. They showed that a small difference in the preparation method leads to a significant modification in the response. Instead of analyzing perturbations of host granular medium, our focus here is on the structural rearrangements of

[a] e-mail: vrhovac@phy.bg.ac.yu

guest grains. Experimentally, we study the dependence of the microstructural properties of percolating grains on some parameters like the packing fraction of host granular medium and the effective gravitational field.

Voronoï tessellation is an important tool in the structural analysis of random media such as glass, packings, foams, cellular solids, proteins, etc. The Voronoï tessellation divides a two-dimensional region occupied by disks into space-filling, nonoverlapping convex polygons. Here, we extend the analysis to packings of percolating disks built by the experimental procedure. We apply the novel concept of *shape factor*, recently introduced by Moucka and Nezbeda [24], to measure in detail the topology of the Voronoï cells during the penetration process. Shape factor is a dimensionless measure of the deviation of the Voronoï cells from circularity. This quantity was recently used to study crystallization of two-dimensional systems, both in simulation [24] and experiment [25]. Since shape factor clearly indicates the presence of domains made up of different Voronoï polygons, it gives a relevant physical picture of competition between less and more ordered domains into packing.

To our knowledge, the present study is the first experimental investigation of complex process of granular penetration. We show, using an optical method developed experimentally, that the microscopic texture of the packing of guest grains is quite sensitive to the details of the initial preparation of host granular packing such as polydispersity and initial packing fraction. We make a quantitative characterization of structural changes in granular packing of percolating grains during the penetration. This analysis is based on the shape factor of the Voronoï polygons. The results show that reorganization of percolating grains depends strongly upon the effective gravity field, which controls the confinement pressure inside the granular packing. Finally, for the case of polydispersity of percolating grains, segregation occurs. During penetration the small guest particles segregate to form two lobes surrounding the large guest grains.

In the following section, we present the experimental set-up and describe the experimental procedures. The experimental results on upward penetration of grains through a granular medium are reported and discussed in Section 3. In the last section, we draw some conclusions.

2 Experimental set-up and procedures

Let us now describe our experimental set-up, which is presented in Figure 1. Experiments were carried out on a 2D granular medium, *i.e.*, the motion of the grains is confined to a plane. The host granular packing is constituted of metallic cylinders contained in a rectangular box made of two parallel glass plates, with an inner gap of thickness 3.4 mm, slightly larger than the height of the cylinders, $h = 3.00 \pm 0.01$ mm. The axes of the cylinders are perpendicular to the low frictional glass plates. The lateral walls of the box, made of duraluminum, delimit a rectangular frame of height $H = 340$ mm and an adjustable width of typically $L = 300$ mm. The box is secured on a heavy plane able to be inclined at different rates by means of a pulley system so that we could set an arbitrary inclination angle θ from the horizontal. The angle of inclination θ is measured by means of a goniometer fixed to the plane.

Fig. 1. Photograph of the experimental set-up.

Two types of host granular systems were studied: monodisperse systems and bidisperse systems. We prepare a bidisperse host granular monolayer of metallic cylinders by mixing small (diameter $d_1 = 4.00 \pm 0.05$ mm) and big ones ($d_2 = 6.00 \pm 0.05$ mm) in order to avoid a regular stacking of the grains. A typical bidisperse host granular packing is composed of roughly 4800 grains in an equal proportion in mass of the two types of cylinders, so that the numbers of small and large cylinders are in proportion of 9 to 4. The cylinders of diameter $d_2 = 6.00 \pm 0.05$ mm were used to prepare monodisperse host packings containing about 4000 grains.

The guest (percolating) grains are cylinders of diameter $d_3 = 5.00 \pm 0.05$ mm, initially located in the long narrow channel with adjustable width (see Fig. 1). The channel is positioned along the central axis of the glass container. The channel is always filled with two identical columns of guest grains. The columns of guest grains are closed at the bottom of the channel by a movable duraluminum piston. The piston is pushed upward in $d_3/4$ steps at a small driving velocity between 0.10 and 0.25 mm/s by a stepping motor. The force that one needs to impose in order to move a metallic piston fluctuates remarkably, but unfortunately we cannot measure it. Due to this external force, the guest grains are moved through channel and penetrate from below into bulk of host particles. After the piston travels a $d_3/4$ distance (step length), it stops

and then we optically analyze the packing of percolating grains. The driving of piston is slow enough to provide that packing stays in the quasistatic regime. In dense quasistatic flows, grains are generally close to the jammed state in which particles are in constant contact [26,27]. Note that the packing is left with an open free upper boundary, so that the pile equilibrium is due to the balance between cylinders weights, contact forces, and wall reactions.

In order to study how the structure of the host packing affects the evolution of the rearrangements of the percolating grains, we performed experiments with two sorts of host packings: disordered packings and partially ordered packings. These packings have different structures and packing fractions depending on how they were prepared. We define the packing fraction ϕ of the granular layer as the ratio of the area of grains to the total area they occupy. Packing fraction ϕ is measured in a rectangular frame at distance $3d_2$ from the lateral walls of the box. Then ϕ is calculated considering the area contribution of each disk to this rectangular region. Disordered packings are prepared by pouring grains onto an initially horizontal glass plate at once. They are then spread with a knife edge until a flat layer is obtained, where the cylinders are randomly deposited without contact between them and at rest. The angle of the plane is then slowly increased up to an angle $\theta = 35°$ or $\theta = 70°$, at constant angular velocity of $\approx 5° \, s^{-1}$. These final inclination angles correspond to a value larger than the static Coulomb angle of friction between the metallic grains and the glass plate, which is around 25°. During the plane rotation, grains therefore freely slide downward and reach a mechanically stable state. This way we control the balance of tangential and normal gravitational force on the layer and thus the contact network (and certainly also force network) inside the granular material. The measured packing fraction of these disordered packings is $\phi_d = 0.79 \pm 0.01$. Moreover, the final packing fraction in the case of monodisperse host medium, composed of the disks of diameter $d_2 = 6.0 \pm 0.1$, has a slightly larger value, $\phi'_d = 0.80 \pm 0.01$.

Partially ordered packings consist of the previous monodisperse random packing but in a compacted form. These packings are obtained by using the same initial procedure followed by vibration of the inclined plane before starting the experiment with a hammer-like device installed below the container. The packing fraction of densely packed systems (referred to as densed or ordered) is $\phi'_o = 0.86 \pm 0.01$, which represents an increase of 7.5% compared to ϕ'_d. Those densities are far from the close packing limit $\phi_{cp} = \pi/2\sqrt{3} \approx 0.91$. The packing fractions have been calculated from an average over 10 initial preparations of host packing.

The experimental study of collective rearrangements of grains requires to get a precise measurement of grain positions. For this reason, the development of an accurate image processing technique has been a central aspect of the design of the experimental set-up. During an experiment, the granular layer is repeatedly scanned by means of HP Scanjet 3800. The scanner is firmly fixed to the plane narrowly below the bottom glass plate of the rectangular container. The scanner frame covers an area of 210×297 mm. The experimental device is isolated from ambient light. We have verified that this apparatus does not produce vibrations which can trigger avalanches or any other motion in the granular layer. The images are systematically acquired after each piston step in resolution 600×600 dpi and 256 gray levels. First, image intensity values are adjusted in order to increase the contrast of the output image. Both the center and the diameter of each grain are accurately determined using the image processing program based on the Standard Hough Transform (SHT) [28]. In the output bitmap image, the diameter of a small and large host grains are $d_1 \approx 94$ and $d_2 \approx 142$ pixels, respectively, and the corresponding value for a guest grains is $d_3 \approx 118$ pixels. This analysis allows one to detect both the centers and the diameters of cylinders with a high resolution of 0.04 mm.

It should be noted that we do not control the ambient humidity of the laboratory. Humidity can lead to the formation of cohesive liquid bridges between granular particles. However, we do not expect the bridges to significantly affect our large 4–6 mm metallic disks.

In the following section we describe some relevant experimental observations.

3 Experimental results and discussion

First, we describe qualitatively the events observed when an experiment is performed for two different inclination angles θ of the plane. Next we characterize quantitatively the structural changes that occur in the packing of guest grains during the penetration for resulting values of the effective gravity $g \sin\theta$ (where g is the gravitational acceleration).

Figure 2 presents four snapshots of the layer at different stages of the experiment for inclination angles $\theta = 35°$ (Fig. 2(a), (c)), and $\theta = 70°$ (Fig. 2(b), (d)). Example snapshots (a) and (b) of the granular layer are taken after injection of 170 guest grains into the host granular mixture. The centers of all guest grains detected by the image processing are marked with red crosshairs. By comparing Figure 2(a) to Figure 2(b), it can be observed that a larger value of the effective gravity $g \sin\theta$ leads to a more compact and a more ordered packing of percolating grains. During the penetration of guest grains, some grains come to equilibrium simultaneously by contacting and supporting each other. These mutually stabilized sets of grains are called arches or bridges [29–31]. Arching is the collective process associated with the appearance of interstitial voids (pores). The total holes area in the packing is also a measure of the compactness. One can see in Figure 2(a) that void spaces are rather nonuniform in size and almost homogeneously distributed throughout the whole packing of guest grains. The packing of percolating grains obtained with $\theta = 70°$ (Fig. 2(b)) is clearly more ordered than the former, showing a localized crystal-like domain on the right side of the packing. Voids are rarer in this case, since the large arches are "destroyed" by increasing the effective gravity.

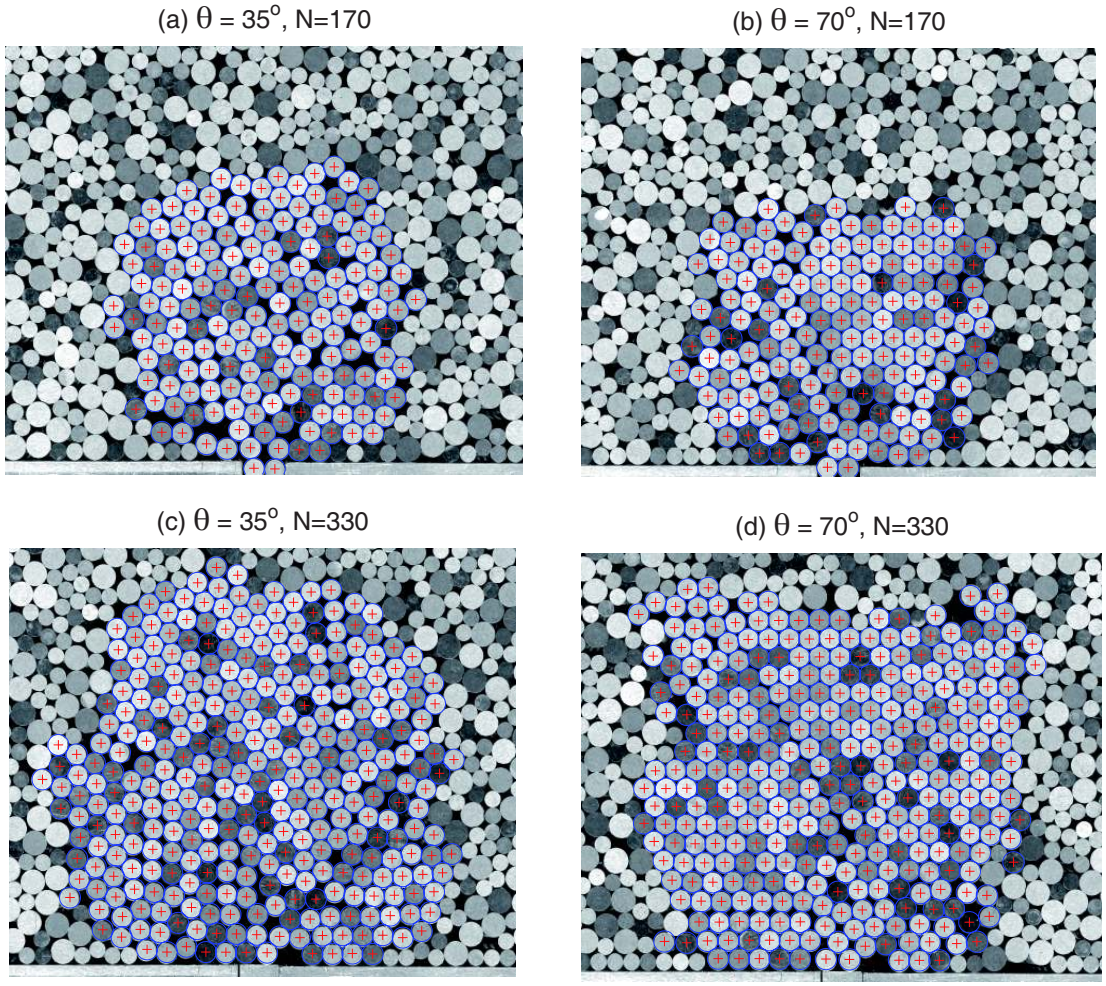

Fig. 2. (Colour on-line) Typical snapshots of a part of packing at inclination angle of (a), (c) $\theta = 35^\circ$, and (b), (d) $\theta = 70^\circ$. The snapshots are taken after injection of (a), (b) $N = 170$, and (c), (d) $N = 330$ guest grains. The centers of all guest grains are marked with red crosshairs.

During the whole process of upward penetration for $\theta = 70^\circ$, the packing of guest grains remains more compact than the packing for $\theta = 35^\circ$. As can be seen in Figure 2(c), for the inclination angle $\theta = 35^\circ$, the packing (c) of 330 guest grains has lot of pores of various sizes. In the case of larger angle $\theta = 70^\circ$ (Fig. 2(d)), the packing (d) containing the same number of guest grains as sample (c) is composed of large dense domains.

The presented results seem to indicate the existence of a correlation between the degree of disorder in the system of percolating grains and the values of the effective gravity $g \sin\theta$. Our aim is to find a more mathematical and quantitative characterization of the structural organization of such systems. The study of how space is shared among the percolating grains is essential for understanding how efficiently the disks are arranged locally. The first problem to address is how to divide the whole space occupied by the granular material into parts associated with the local environment around each disk. The natural way to subdivide space into smaller portions is Voronoï Tesselation (VT) [32]. For a given two-dimensional distribution of disks VT is a uniquely defined set of convex cells, each of which encloses one and only one of these disks. A Voronoï cell (polygon in 2D) associated with a disk is defined as an assembly of points which are closer to that disk than to any of the other disks in the packing. Two disks sharing a common cell edge are neighbors. Each vertex of this tessellation is equidistant to three neighboring disks. The individual characteristics of Voronoï cells as, *e.g.*, the number of edges, circumference, surface, etc., are not able to characterize in detail tiny structural effects [33,34] and have very poor sensitivity to the packing properties [35]. However, a better indicator of structural changes is the shape factor ζ (parameter of nonsphericity) which combines the circumference C and the surface S of Voronoï cells [24,36], which we define by

$$\zeta = \frac{C^2}{4\pi S}\,. \tag{3.1}$$

For a circle, this coefficient is equal to 1. For a convex polygon, the more anisotropic the polygon, the higher is $\zeta > 1$. For a square $\zeta = 4/\pi \approx 1.273$, for a regular pentagon $\zeta = \pi/5\tan(\pi/5) \approx 1.156$, and for a regular hexagon $\zeta = 6/\sqrt{3\pi^2} \approx 1.103$.

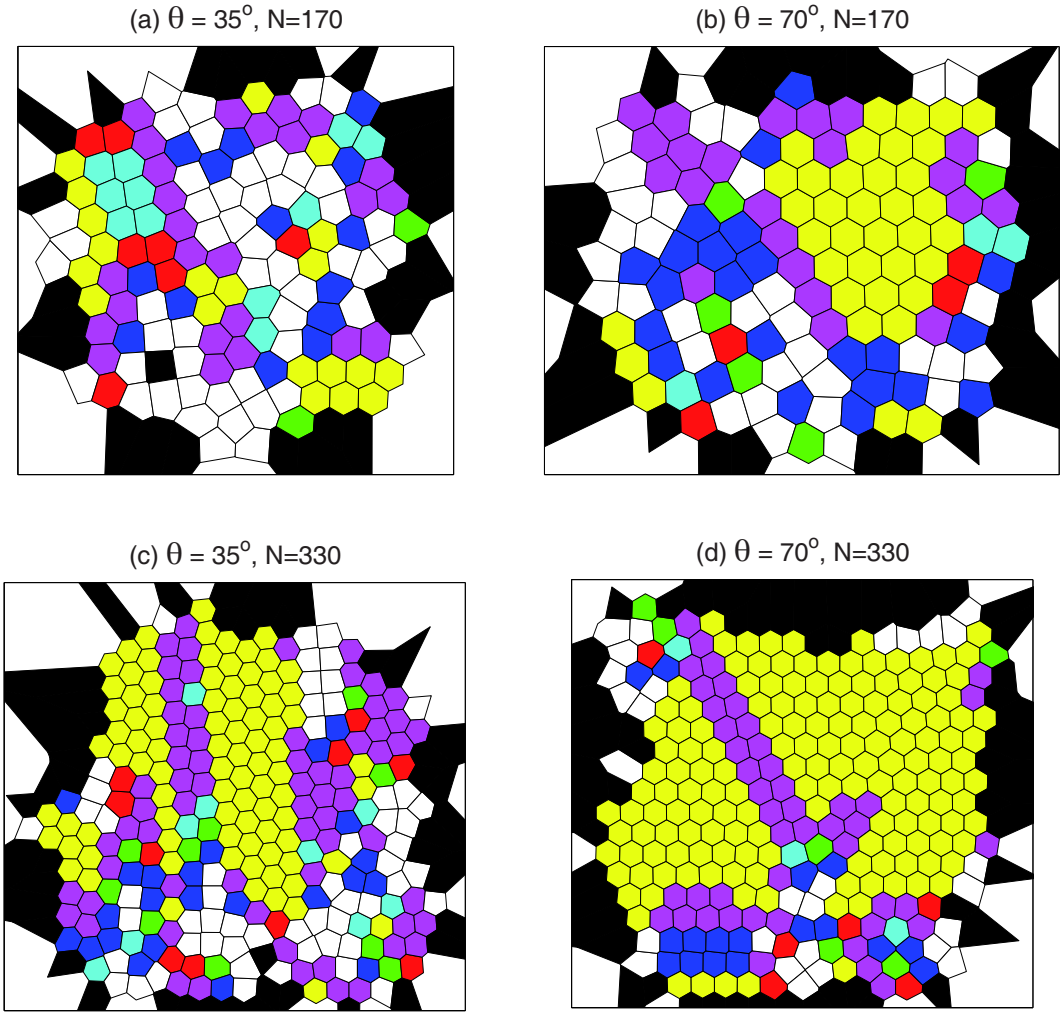

Fig. 3. (Colour on-line) Voronoï diagrams obtained from the positions of the percolating disks, for the same disks configurations as in Figure 2. Voronoï cells are colored according to their shape factor ζ (Eq. (3.1)). Color coding of Voronoï polygons is defined in Table 1.

The shape factor is able to identify the occurrence of different domains in experimentally obtained packings of guest particles. Every domain is made up of grains whose Voronoï polygons have similar values of the shape factor. Note that the distribution of the shape factor (the occurrence probability of different polygons) for the fluid of two-dimensional hard disks depends on the packing fraction [24]. For densities corresponding to the packings presented in Figure 2, the distribution of ζ diminishes above ≈ 1.25. To clearly distinguish domains made up of different Voronoï polygons, we classify in Table 1 the polygons according to their ζ values into eight groups, G_1–G_8. Group G_1 comprises near-regular hexagons, while other groups include less regular (round) figures.

In Figure 3 we show the Voronoï tessellation of a packing of percolating disks for the same series of disks configurations as in Figure 2. To differentiate polygons belonging to different groups G_1–G_8, we use color coding in accordance with the definitions given in the Table 1.

Table 1. The table summarizes the classification of Voronoï polygons into eight groups G_1–G_8 according to the values of the shape factor ζ (Eq. (3.1)).

Group	Range	Colour
G_1	$\zeta < 1.108$	yellow
G_2	$1.108 < \zeta < 1.125$	magenta
G_3	$1.125 < \zeta < 1.130$	cyan
G_4	$1.130 < \zeta < 1.135$	red
G_5	$1.135 < \zeta < 1.140$	green
G_6	$1.140 < \zeta < 1.160$	blue
G_7	$1.160 < \zeta < 1.250$	white
G_8	$1.250 < \zeta$	black

This allows us to easily distinguish local arrangements of percolating grains for used packings. In Figure 3(a) we observe a mixture of various Voronoï polygons. It is obvious

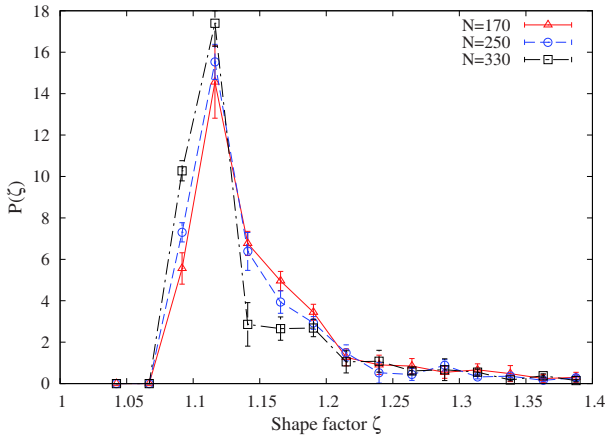

Fig. 4. Evolution of the probability distribution $P(\zeta)$ of the shape factor ζ for the packing of percolating disks during injection. Experimental points are related to the various numbers of guest grains N: $N = 170$ ($\triangle$), $N = 250$ ($\bigcirc$), and $N = 330$ ($\square$). The results correspond to the plane inclination of $\theta = 70°$. The error bars denote the standard deviation of the data. The lines are guides to the eye.

that figures belonging to class G_7 dominate, where G_7 polygons are mostly distorted pentagons. Only small islands of near-regular hexagons belonging to class G_1 are found. Moreover, small domains made up of G_2–G_6 polygons, respectively, can also be detected. It means that the percolating disks are distributed quite randomly and no specific configurations of disks are formed. As the number of percolating grains increases further (Fig. 3(c)), more regular cells can be observed and their occurrence starts prevailing, though the structure of the system is still disordered. There are still a few disordered regions within the system of percolating grains. However, in the case of a larger value of the effective gravity (Fig. 3(b)) we find large domain made up predominantly of more or less regular hexagons (figures belonging to classes G_1 and G_2). This cluster grows rapidly with a further increase of the number of guest grains inside the container. Ultimately, for $\theta = 70°$, the system of percolating grains ends up in configurations where large clusters of near-regular Voronoï cells (class G_1) are found (Fig. 3(d)). As one could expect, regions of more distorted Voronoï cells (G_4–G_7) are mainly located near the entrance of guest grains.

In order to better quantify the structural changes in the packings of percolating grains presented above, we consider here the probability distribution $P(\zeta)$ of the shape factor ζ. The distribution function $P(\zeta)$ is related to the probability of finding the Voronoï cell with shape factor ζ. It is normalized to unity, namely, $\int_0^\infty \mathrm{d}\zeta P(\zeta) = 1$. Fluctuations in the measurements of $P(\zeta)$ are reduced by averaging over ten different experiments, performed under the same conditions. Figure 4 compares the probability distribution $P(\zeta)$ for packings of $N = 170$, 250, and 330 guest grains. One can see that the distribution $P(\zeta)$ tends to narrow during the upward penetration of guest grains. This narrowing of the probability distribution $P(\zeta)$ corresponds to a decrease of the fraction of Voronoï polygons belonging to classes G_5–G_7.

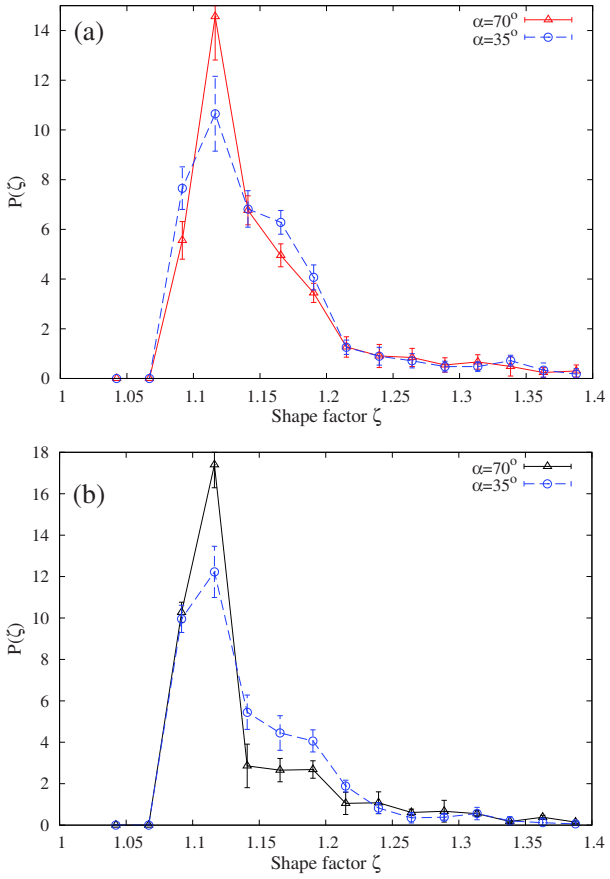

Fig. 5. Probability distribution $P(\zeta)$ of the shape factor ζ for the packings of percolating disks in dependence on the effective gravity at different stages of the experiment: (a) $P(\zeta)$ after injection of $N = 170$ guest disks; (b) $P(\zeta)$ after injection of $N = 330$ guest disks. Triangles ($\triangle$) and circles ($\bigcirc$) correspond to inclination angles of $\theta = 70°$ and $\theta = 35°$, respectively. The error bars denote the standard deviation of the data. The lines are guides to the eye.

In Figure 5 we compare the function $P(\zeta)$ for the two values of inclination angle $\theta = 70°, 35°$. Figure 5(a) shows the corresponding results for $P(\zeta)$ after injection of 170 guest disks into bidisperse host granular medium. One can see that the probability distribution $P(\zeta)$ becomes narrower and more localized around the maximum as the effective gravity (inclination angle θ) increases. In other words, the Voronoi cells become more circular at higher values of effective gravity. As the number of guest grains is increased further to $N = 330$ (Fig. 5(b)), contribution of less circular cells to the distribution function $P(\zeta)$ decreases for both the 70° and 35° inclination angles.

Additionally, in order to characterize the upward penetration of grains quantitatively, we also analyzed the mobility of guest grains for the different values of the effective gravity. The mobility is a kinematic property of the system associated with the motion of guest grains in their nearest neighborhood inside the packing, under the action of gravitation force and external force induced by the moving piston. We concentrate here on the drift of the grains that can occur in the direction of effective gravity. Consequently,

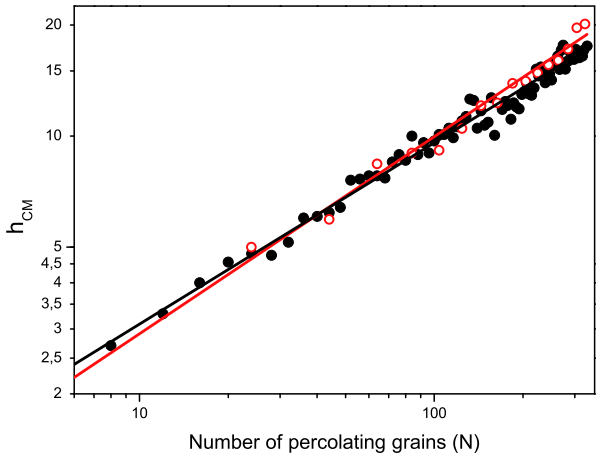

Fig. 6. (Colour on-line) The average height $h_{\rm CM}$ of the center of mass of the system of percolating grains increases algebraically with the number of percolating disks. Empty (red) and full (black) symbols correspond to inclination angles $\theta = 35^\circ$ and $\theta = 70^\circ$, respectively. The continuous superimposed lines are fits according to equation (3.3). The unit of the height $h_{\rm CM}$ is set to the grain radius d_3. The error bars on the values of $h_{\rm CM}$ are of the order ± 0.5.

we analyze the evolution of the average height $h_{\rm CM}$ of the center of mass of the system of guest grains, which is defined as

$$h_{\rm CM}(N) = \frac{1}{N}\sum_{i=1}^{N}\frac{\langle h_i\rangle}{d_3}\,, \qquad (3.2)$$

where N is the number of guest particles inside the container, h_i is the perpendicular distance of the i-th guest grain from the bottom of the rectangular container and the angular brackets denote an average over independent experiments (typically eight). The parameter $h_{\rm CM}(N)$ increases with number of percolating disks N inside the container as shown in Figure 6. The parameter $h_{\rm CM}(N)$, for a given value of inclination angle θ, seems to be a simple power law of the number of guest grains N

$$h_{\rm CM}(N) = A\, N^{\gamma}. \qquad (3.3)$$

The higher value of the effective gravity ($\theta = 70^\circ$) leads to a slightly lower exponent $\gamma = 0.49 \pm 0.01$ of power law (3.3), than the lower value of the effective gravity ($\theta = 35^\circ$), for which $\gamma = 0.53 \pm 0.01$. We have obtained that $A = 19.9 \pm 0.1$, 17.0 ± 0.1 for $\theta = 70^\circ$, 35°, respectively. The dependence of $h_{\rm CM}$ on the number of guest particles N can be deduced by a simple dimensional analysis. The surface of the guest packing is proportional to N. For the symmetric spreading of the packing of injected grains, $h_{\rm CM}$ is proportional to the square root of the surface. Hence, $h_{\rm CM} \propto N^{1/2}$, which is consistent with the scaling relation (3.3) obtained in the experiment.

Previous findings (Figs. 2–6) suggest that a host granular material in the case of the higher values of the effective gravity is macroscopically stronger. The increased reaction of host granular packing to the penetrating grains is due to the greater resistance of force network to the perturbations. This is in agreement with experiments and numerical simulations examining the effect of packing density and gravity on the force network [17,37–39]. As gravity decreased, or, as packing fraction increased, the spatial distribution of the force chain network changed from a dense, tangled network to one consisting of less tangled, longer chains [38]. Intuitively, we would expect longer chains to be less stable. In addition, shorter chains can support greater stress since there are fewer potential failure points [17,40]. This suggests that granular packings with shorter chains are macroscopically stronger than those with longer chains. Also, packings with more branching in their force chain network are macroscopically stronger, since there are more pathways available for stress transmission. Thus, shorter force chains and a greater degree of branching in the force chain network, induced by higher values of the effective gravity [38], result in macroscopically stronger host granular packing.

Another important feature is the dependence of upward penetration of the grains on the packing fraction ϕ of the host granular medium. We perform these experiments on two different types of monodisperse random packings described previously in Sect. 2: the "disordered" (noncompact) and "partially ordered" (compacted) host packing. The results of the experiments made with a noncompact host granular medium are shown in Figures 7(a) and (c). Figure 7(a) shows the snapshot when 170 grains are injected into the host granular packing. We observe that some of the guest disks start to order, though the structure of the system is still predominantly disordered. Increasing the number of guest grains further takes the system from this disordered configuration through the phase of gradual building of a regular hexagonal arrangement to a solid-like structure (Fig. 7(c)). These observations are also confirmed by our analysis of shapes of the Voronoï cells shown in Figures 8(a) and (c). Indeed, in Figure 8(c) the overwhelming majority of the disks form near-regular hexagons which indicates that most of the guest disks are in solid-like, ordered domains.

With the compacted host granular medium we made the same experiments. The results are qualitatively similar as seen in Figures 7(b) and (d). The corresponding snapshots of the network of Voronoï cells shaded according to their circularity ζ (see Tab. 1) are presented in Figures 8(b) and (d). For $N = 338$ guest grains we find two large domains made up of Voronoï polygons belonging to class G_1. These blocks are clearly separated by a thin disordered region because rupture occurs inside the compact blocks of percolating grains.

Figure 9 displays two plots of probability distribution $P(\zeta)$ of the shape factor ζ, which correspond to penetration of guest grains into disordered ($\phi = 0.80$) and partially ordered ($\phi = 0.86$) host granular packings. In the case of penetration into disordered host granular packing, the granular layer consists almost entirely of guest particles whose Voronoï cells are regular hexagons and crystallization occurs. We thus get a very narrow probability distribution $P(\zeta)$ centered at $\zeta \approx 1.1$ (the value for regular hexagons). However, in the case of penetration into compacted host granular medium, the probability distribution

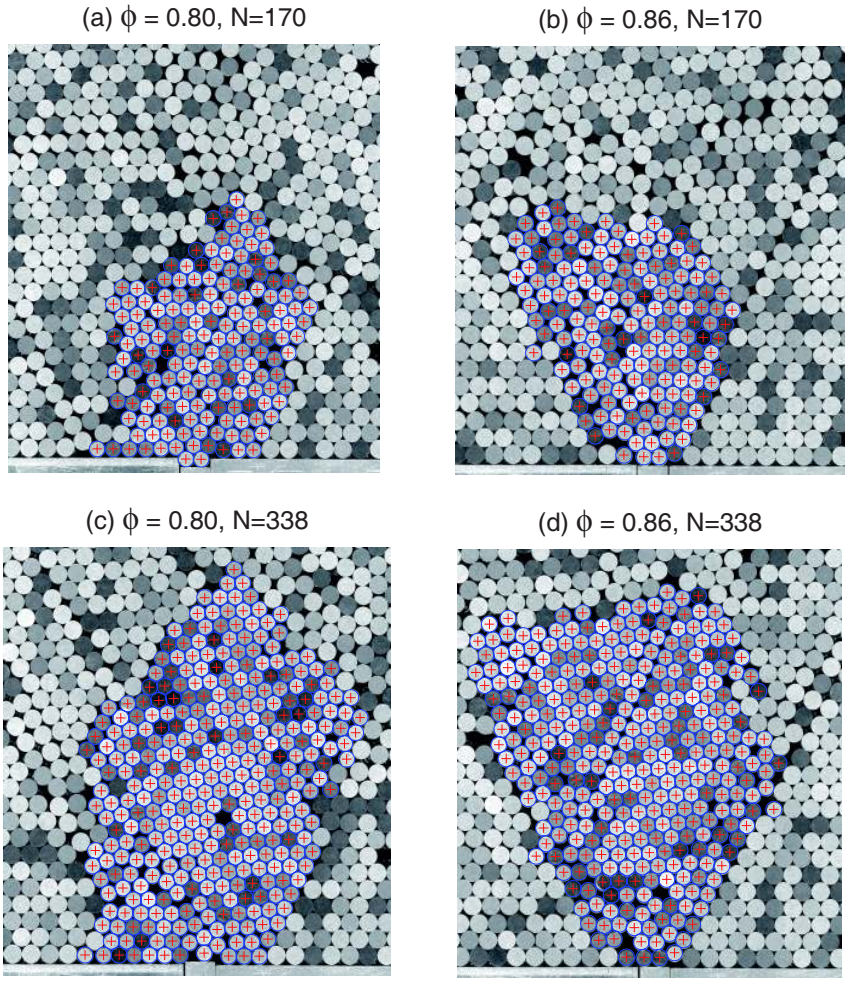

Fig. 7. (Colour on-line) Typical snapshots of a part of packing at the initial packing fraction of host granular media of (a), (c) $\phi = 0.80$, and (b), (d) $\phi = 0.86$. The snapshots are taken after injection of (a), (b) $N = 170$, and (c), (d) $N = 338$ guest grains. The centers of all guest grains are marked with red crosshairs.

$P(\zeta)$ clearly shows the existence of two distinct classes of Voronoï shapes. Low ζ maximum in the probability distribution $P(\zeta)$ is caused by six-sided regular cells. A second maximum in $P(\zeta)$ (centered at $\zeta \approx 1.16$) is caused by the overlapping contribution of distorted hexagons and pentagons. Examining the above snapshoots (see, *e.g.* Fig. 8(d)) shows that these distorted cells mainly come from grains located in stretched regions between large solid-like domains.

The main difference with the experiments with a bidisperse host granular medium is the anisotropy of penetration. Here, anisotropy refers to the different depths to which the guest particles penetrate into the host packing, depending on the spatial direction. Anisotropy is larger in the monodisperse case when we observe the strongly asymmetric spreading of the cluster of injected grains. A possible reason for this is the difference in the distribution of coordination numbers for monodisperse and polydisperse systems [41]. The distribution of coordination numbers for polydisperse systems is more spread, which provides a force chain network with more branch points. In the systems with more branching in their force chain network there are more pathways available for stress transmission. In contrast, monodisperse packings are limited in their range of coordination numbers, which limits possible directions for force transmission. This suggests that a host granular material ability to form straight chains [17] is one factor that governs anisotropy of penetration of guest particles.

Compaction of host granular packing also increases anisotropy of penetration of guest grains. By visualizing the host medium rearrangement, the origin of this anisotropy is clearly identified. It is well known that monodisperse two-dimensional packings of disks exhibit a spontaneous tendency to order [42]. In two dimensions, when equal discs are poured in a disorderly fashion into a container, they tend to organize themselves locally into close-packing configurations. Shaking can increase the packing fraction, leading gradually to an overall ordered configuration. Such a local organization is extended over long distances yielding assemblies with privileged paths for force propagation. Local recrystallization provides that monodisperse packings have straighter force chains, since in crystallized regions long chains are almost perfectly

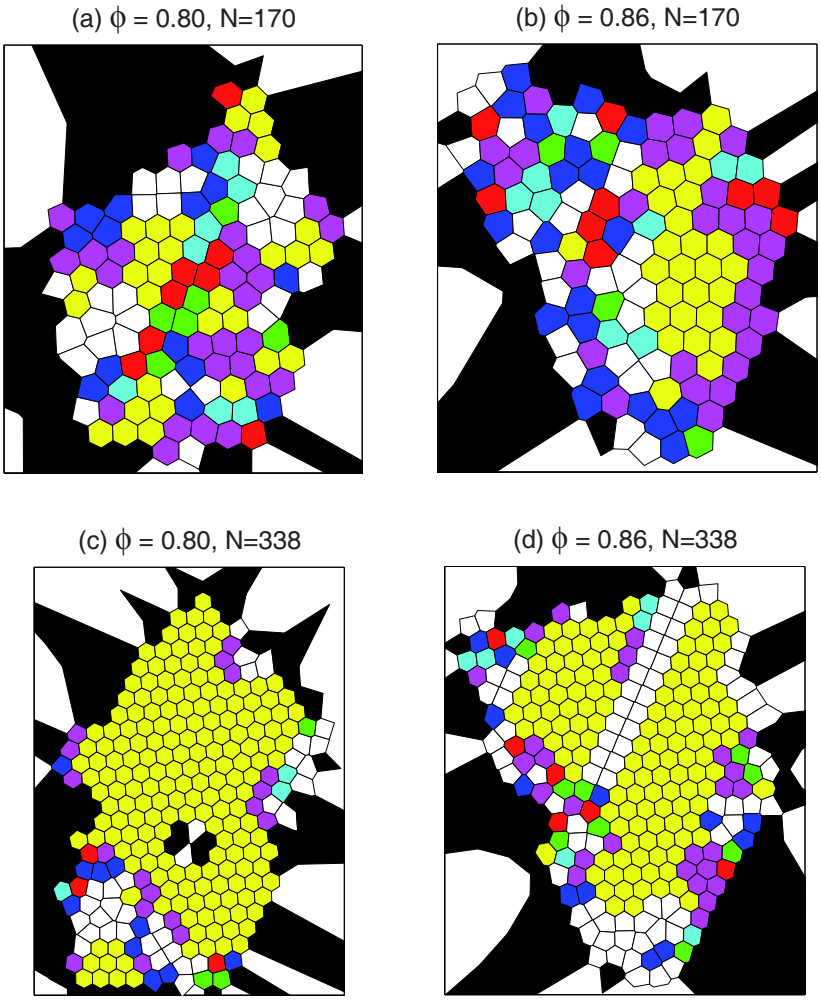

Fig. 8. (Colour on-line) Voronoï diagrams obtained from the positions of the percolating disks, for the same disks configurations as in Figure 7. Voronoï cells are colored according to their shape factor ζ (Eq. (3.1)). The color coding of Voronoï polygons is defined in Table 1.

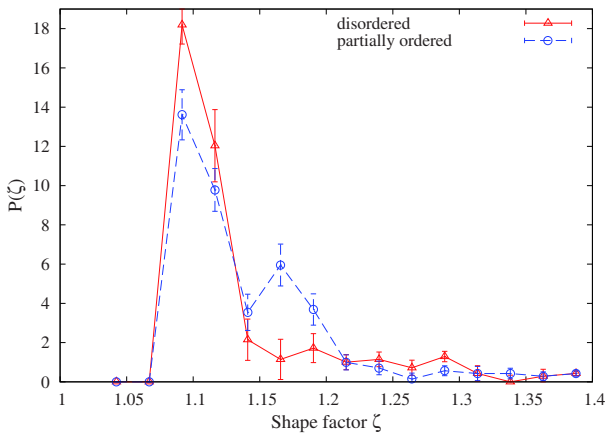

Fig. 9. Probability distribution $P(\zeta)$ of the shape factor ζ after injection of $N = 338$ guest grains into disordered ($\triangle$) and partially ordered ($\bigcirc$) host packing. The results correspond to the plane inclination of $\theta = 35^\circ$. The error bars denote the standard deviation of the data. The lines are guides to the eye.

straight. As a consequence, the internal deformation process of monodisperse host packing occurs via the nucleation and the propagation of one or several "cracks" defining separate blocks of grains which move as a whole. These cracks are preferentially initiated by piling defects. Clusters of particles eventually break down and new ones are formed as guest grains penetrate. Optical imaging brings evidence that the anisotropy of penetration of guest grains is associated with crack formations inside the host granular medium.

We next present measurements of upward penetration of a granular mixture through a mono-disperse host granular medium. Experiments are performed using a $50\% : 50\%$ mixture of small and large cylindrical grains with diameters $d_1 = 4.00 \pm 0.05\,\mathrm{mm}$ and $d_2 = 6.00 \pm 0.05\,\mathrm{mm}$, respectively. The host packing is made of monodisperse cylinders of diameter $d_3 = 5.00 \pm 0.05\,\mathrm{mm}$. The guest grains are initially placed above the piston in a long channel of width $d_{\mathrm{ch}} \gtrapprox d_1 + d_2$. The channel is filled with two columns of guest grains. Small and large grains

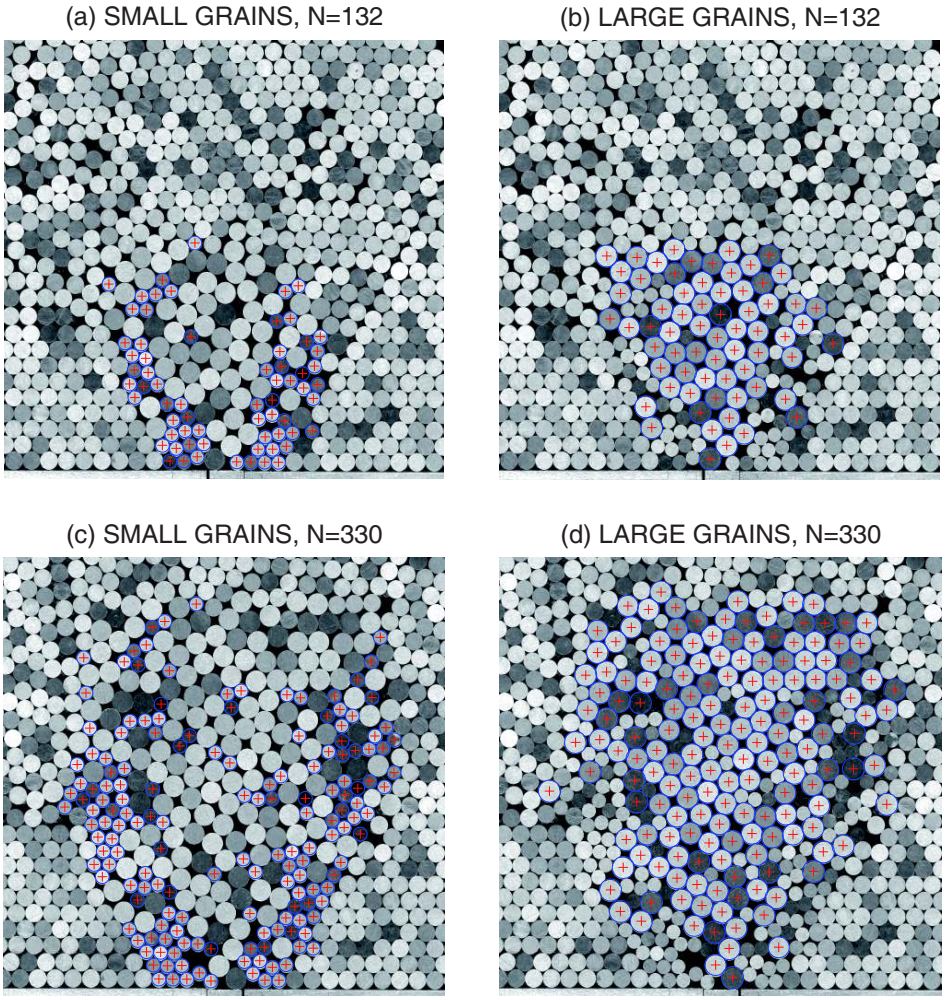

Fig. 10. (Colour on-line) Segregation is observed when a mixture of granular grains differing in size is injected into a monodisperse host granular packing. The two typical snapshots are taken after injection of (a), (b) $N = 132$, and (c), (d) $N = 330$ guest grains. Centers of small (large) guest grains are marked with red crosshairs in pictures (a) and (c) ((b) and (d)).

are placed in alternate order along each column. Consequently, the system of guest grains inside the channel can be considered as an initially homogeneous granular mixture.

Representative segregation patterns of the granular layer taken after injection of 132 and 330 guest grains into a monodisperse host granular medium are presented in Figures 10(a) and (c), respectively. The centers of all small guest grains detected by the image processing are marked with red crosshairs. The same snapshots are presented in Figures 10(b) and (d), where only centers of large guest grains are marked. By comparing the corresponding snapshots given in Figure 10, it can be observed that the mixture of guest grains self-organizes partially during the upward penetration. Small particles segregate to form two lobes surrounding the large guest grains. The segregation is imperfect. Small percolating grains are interspersed among large guest grains.

This segregation can be explained by a simple geometrical mechanism [11]. During the quasistatic flow guest particles move upwards, but small particles have a larger probability to drop down through the suitable voids than large particles. This leads to the small particles falling through the interstices between the larger particles. Small particles preferentially accumulate near the boundary between large guest grains and host granular medium because host packing is more compacted than packing of large guest grains. The net result of the percolation of smaller particles through the voids in the lattice of larger guest particles is the formation of a core having two regions rich in small particles near the inlet at the bottom of the container, as shown in Figure 10(a). As can be seen from Figure 10(c), these regions continue to grow up during the upward penetration of guest grains into the lobe-shaped patterns. The lobes stretch along the boundary between large guest grains and the host granular medium, and appear to be nearly symmetric about the vertical midline.

4 Concluding remarks

We presented an experimental report on structural changes of granular packing during the creeping (quasi-

static) penetration of grains through a dense granular medium. The granular organization at local level was studied by analyzing the shape factor ζ (Eq. (3.1)) of the local volumes associated with a natural way of subdividing the volume into local parts —the Voronoï partition. The shape factor ζ is a quantifier of the circularity of Voronoï cells associated with the individual particles. It gives a clear physical picture of competition between less and more ordered domains of guest particles during penetration.

The scenario of the evolution of the percolating grains depends on both the polydispersity and the initial packing fraction of the host grains. In this paper, we have attempted to give insights into mechanisms by which these packing properties handle grain penetration. Anisotropy of penetration is larger in the monodisperse case than in the bidisperse one, for the same value of the packing fraction of the host medium. It was shown that compaction of host granular packing also increases the anisotropy of penetration of guest grains. We have related this anisotropy with crack formations inside the host granular medium, which are a consequence of the fragile nature of granular material.

We have shown that granular penetration dynamics is sensitive to the effective gravity. Generally, higher effective gravity increases the resistance to upward penetration and enhances the structural organization in the system of the percolating grains. Experimental results show that the vertical position of the center of mass of the percolating grains increases algebraically with their number inside the container. Our results are rather consistent with observations from experiments and numerical simulations that examined the features of force chain network [17, 37–39]. Findings indicate that increasing effective gravity induces the formation of macroscopically stronger host granular media. In fact, the increased bulk resistance of host medium to the grain penetration is a consequence of the formation of shorter force chains and greater degree of branching in the force chain network.

We have experimentally investigated the penetration of mixtures of large and small particles through a monodisperse host granular medium. We have shown that particle polydispersity of percolating grains leads to size segregation. In the partially segregated state, small percolating particles surround the larger guest particles. The simple model of process of segregation [11] based on the diameters of each disk, and their probabilities of finding a hole of their size, is sufficient to explain the observed features of segregation.

Nevertheless, the results presented here provide the starting point for further investigations. Further experiments are needed to understand other factors that influence the penetration of grains such as particle anisotropy, particle shape and frictional properties of the grains. Another promising direction of research concerns the 3D extension of this investigation. But, one has to be careful in extending the conclusions to three dimensions. For example, our results suggest that the competition between the tendency to form locally compact configurations in the packing and the geometrical frustration could be the key to understanding the mechanism of process of granular penetration. However, it is known that the tendency toward a crystalline order is much less spontaneous in three dimensions than in the two-dimensional case [42]. Furthermore, the dimensionality of the packing determines the nature of the tail of the probability density of contact forces inside the packing [43], which is also relevant to the process of granular penetration.

This research was supported by the Ministry of Science of the Republic of Serbia, under Grants Nos. OI141003 and OI141035.

References

1. L.P. Kadanoff, Rev. Mod. Phys. **71**, 435 (1999).
2. I. Goldhirsch, Annu. Rev. Fluid Mech. **35**, 267 (2003).
3. O. Pouliquen, Phys. Fluids **11**, 542 (1998).
4. L.E. Silbert, D. Ertas, G.S. Grest, T.C. Halsey, D. Levine, S.J. Plimpton, Phys. Rev. E **64**, 051302 (2001).
5. O. Pouliquen, Phys. Rev. Lett. **93**, 248001 (2004).
6. L.E. Silbert, Phys. Rev. Lett. **94**, 098002 (2005).
7. W. Losert, L. Bocquet, T.C. Lubensky, J.P. Gollub, Phys. Rev. Lett. **85**, 1428 (2000).
8. K.E. Daniels, R.P. Behringer, Phys. Rev. Lett. **94**, 168001 (2005).
9. K.M. Hill, A. Caprihan, J. Kakalios, Phys. Rev. Lett. **78**, 50 (1997).
10. A. Kudrolli, Rep. Prog. Phys. **67**, 209 (2004).
11. M. Schröter, S. Ulrich, J. Kreft, J.B. Swift, H.L. Swinney, Phys. Rev. E **74**, 011307 (2006).
12. J.B. Knight, C.G. Fandrich, C.N. Lau, H.M. Jaeger, S.R. Nagel, Phys. Rev. E **51**, 3957 (1995).
13. P. Philippe, D. Bideau, Europhys. Lett. **60**, 677 (2002).
14. P. Ribière, P. Richard, D. Bideau, R. Delannay, Eur. Phys. J. E **16**, 415 (2005).
15. G. Lumay, N. Vandewalle, Phys. Rev. Lett. **95**, 028002 (2005).
16. D. Arsenović, S.B. Vrhovac, Z.M. Jakšić, Lj. Budinski-Petković, A. Belić, Phys. Rev. E **74**, 061302 (2006).
17. M. Muthuswamy, A. Tordesillas, J. Stat. Mech. P09003 (2006).
18. M.B. Stone, R. Barry, D.P. Bernstein, M.D. Pelc, Y.K. Tsui, P. Schiffer, Phys. Rev. E **70**, 041301 (2004).
19. E. Kolb, J. Cviklinski, J. Lanuza, P. Claudin, E. Clément, Phys. Rev. E **69**, 031306 (2004).
20. B. Francois, F. Lacombe, H.J. Herrmann, Phys. Rev. E **65**, 031311 (2002).
21. G. Caballero, E. Kolb, A. Lindner, J. Lanuza, E. Clément, J. Phys.: Condens. Matter **17**, S2503 (2005).
22. E. Kolb, C. Goldenberg, S. Inagaki, E. Clément, J. Stat. Mech. P07017 (2006).
23. M.R. Shaebani, T. Unger, J. Kertész, Phys. Rev. E **76**, 030301(R) (2007).
24. F. Moučka, I. Nezbeda, Phys. Rev. Lett. **94**, 040601 (2005).
25. P.M. Reis, R.A. Ingale, M.D. Shattuck, Phys. Rev. Lett. **96**, 258001 (2006).
26. S. McNamara, R. García-Rojo, H.J. Herrmann, Phys. Rev. E **72**, 021304 (2005).
27. S. McNamara, H.J. Herrmann, Phys. Rev. E **74**, 061303 (2006).
28. B. Drew, *Hough transform*, From MathWorld–A Wolfram Web Resource, created by Eric W. Weisstein. `http://mathworld.wolfram.com/HoughTransform.html`.

29. A. Mehta, G.C. Barker, J.M. Luck, J. Stat. Mech. P10014 (2004).
30. L.A. Pugnaloni, M.G. Valluzzi, L.G. Valluzzi, Phys. Rev. E **73**, 051302 (2006).
31. R. Arévalo, D. Maza, L.A. Pugnaloni, Phys. Rev. E **74**, 021303 (2006).
32. F. Aurenhammer, ACM Computing Surveys **23**, 345 (1991).
33. D.P. Fraser, M.J. Zuckermann, O.G. Mouritsen, Phys. Rev. A **42**, 3186 (1990).
34. A. Huerta, G.G. Naumis, Phys. Rev. Lett. **90**, 145701 (2003).
35. P. Richard, L. Oger, J.P. Troadec, A. Gervois, Phys. Rev. E **60**, 4551 (1999).
36. P. Richard, J.P. Troadec, L. Oger, A. Gervois, Phys. Rev. E **63**, 062401 (2001).
37. D. Howell, R.P. Behringer, C. Veje, Phys. Rev. Lett. **82**, 5241 (1999).
38. M. Muthuswamy, A. Tordesillas, in *Proceedings of the 10th ASCE Aerospace Division International Conference on Engineereng, Construction and Operations in Challenging Environments (Earth & Space 2006)*, edited by R.B. Malla, W.K. Binienda, A.K. Maji (Aerospace Division of the American Society of Civil Engineers, Reston, VA, 2006) p. 33.
39. A. Modaressi, S. Boufellouh, P. Evesque, Chaos **9**, 523 (1999).
40. J.L. Anthony, C. Marone, J. Geophys. Res. **110**, B08409 (2005).
41. C. Voivret, F. Radjaï, J.-Y. Delenne, M.S. El Youssoufi, Phys. Rev. E **76**, 021301 (2007).
42. T. Aste, J. Phys.: Condens. Matter **17**, S2361 (2005).
43. A.R.T. van Eerd, W.G. Ellenbroek, M. van Hecke, J.H. Snoeijer, T.J.H. Vlugt, Phys. Rev. E **75**, 060302(R) (2007).